



The FRB 121102 Host Is Atypical among Nearby Fast Radio Bursts

Ye Li^{1,2}, Bing Zhang³, Kentaro Nagamine^{4,3,5}, and Jingjing Shi¹

¹Kavli Institute for Astronomy and Astrophysics, Peking University, Beijing 100871, People's Republic of China

²Purple Mountain Observatory, Chinese Academy of Sciences, Nanjing 210008, People's Republic of China

³Department of Physics and Astronomy, University of Nevada, Las Vegas, NV 89154, USA

⁴Theoretical Astrophysics, Department of Earth and Space Science, Graduate School of Science, Osaka University, 1-1 Machikaneyama, Toyonaka, Osaka 560-0043, Japan

⁵Kavli-IPMU (WPI), University of Tokyo, 5-1-5 Kashiwanoha, Kashiwa, Chiba, 277-8583, Japan

Received 2019 June 20; revised 2019 August 1; accepted 2019 August 23; published 2019 October 11

Abstract

We search for host galaxy candidates of nearby fast radio bursts (FRBs), FRB 180729.J1316+55, FRB 171020, FRB 171213, FRB 180810.J1159+83, and FRB 180814.J0422+73 (the second repeating FRB). We compare the absolute magnitudes and the expected host dispersion measure DM_{host} of these candidates with that of the first repeating FRB, FRB 121102, as well as those of long gamma-ray bursts (LGRBs) and superluminous supernovae (SLSNe), the proposed progenitor systems of FRB 121102. We find that while the FRB 121102 host is consistent with those of LGRBs and SLSNe, the nearby FRB host candidates, at least for FRB 180729.J1316+55, FRB 171020, and FRB 180814.J0422+73, either have a smaller DM_{host} or are fainter than FRB 121102 host, as well as the hosts of LGRBs and SLSNe. In order to avoid the uncertainty in estimating DM_{host} due to the line-of-sight effect, we propose a galaxy-group-based method to estimate the electron density in the intergalactic regions, and hence, DM_{IGM} . The result strengthens our conclusion. We conclude that the host galaxy of FRB 121102 is atypical, and LGRBs and SLSNe are likely not the progenitor systems of at least most nearby FRB sources. The recently reported two FRB hosts differ from the host of FRB 121102 and also the host candidates suggested in this paper. This is consistent with the conclusion of our paper and suggests that the FRB hosts are very diverse.

Unified Astronomy Thesaurus concepts: [High energy astrophysics \(739\)](#); [Radio astronomy \(1338\)](#); [Radio transient sources \(2008\)](#); [Radio bursts \(1339\)](#)

1. Introduction

Fast radio bursts (FRBs) are bright objects in radio, with durations of a few milliseconds (Lorimer et al. 2007; Thornton et al. 2013; Spitler et al. 2014; Petroff et al. 2016, see Lorimer 2018 for a review). The values of their dispersion measure (DM), an indicator of the electron column density along the line of sight, are much larger than the predicted values from the Milky Way galaxy, so they are expected to be of an extragalactic origin.

The origin of FRBs is highly debated. It is known that at least some FRB sources produce repeating bursts (Spitler et al. 2016; CHIME/FRB Collaboration et al. 2019a). These FRBs are usually explained within the “intrinsic” models that invoke young pulsars (Connor et al. 2016; Cordes & Wasserman 2016; Katz 2016), or magnetars (Beloborodov 2017; Kashiyama & Murase 2017; Metzger et al. 2017, 2019), with the ultimate energy coming either from the spindown power or the magnetic power of a neutron star. Alternatively, some “extrinsic” models invoking the kinetic energy of an external source (e.g., the so-called “cosmic comb” model, Zhang 2017, 2018b) or the gravitational energy of an external object (e.g., asteroids hitting neutron stars; Geng & Huang 2015; Dai et al. 2016) have also been discussed in the literature. It is possible that not all FRB sources repeat (Palaniswamy et al. 2018; Caleb et al. 2019). If this is the case, there might be FRBs produced from catastrophic events, such as compact star mergers (Piro 2012; Kashiyama et al. 2013; Totani 2013; Liu et al. 2016; Wang et al. 2016b; Zhang 2016, 2019; Dai 2019) and collapse of supramassive neutron stars to black holes (Falcke & Rezzolla 2014; Zhang 2014).

The extragalactic origin of FRBs is confirmed by the precise localization of the first repeating FRB 121102 (Spitler et al. 2014, 2016; Marcote et al. 2017) and the identification of its host galaxy (Bassa et al. 2017; Chatterjee et al. 2017; Kokubo et al. 2017; Tendulkar et al. 2017). The host galaxy of FRB 121102 is an irregular, low-metallicity dwarf galaxy. FRB 121102 resides in the bright star-forming region in the galaxy. The properties of the host and the subgalactic localization of the source are similar to those of long gamma ray bursts (LGRBs) and superluminous supernova (SLSNe), some of which have been suggested to leave behind rapidly spinning magnetars. As a result, young magnetars born from massive star core collapse events that produced LGRBs or SLSNe are regarded as the leading candidates to power FRBs, and it has been expected that the host galaxy of FRB 121102 should be typical for FRB sources (Bassa et al. 2017; Nicholl et al. 2017).

The search for host galaxies of other FRBs has been carried out. FRB 150418 was proposed to be associated with a fading radio transient, which is located in an elliptical galaxy (Keane et al. 2016). However, the association is not secure because the radio counterpart is a radio persistent source with significant variability (Akiyama & Johnson 2016; Li & Zhang 2016; Vedantham et al. 2016; Williams & Berger 2016; Johnston et al. 2017). Mahony et al. (2018) searched for the host galaxy of FRB 171020 with a small DM (which means it is nearby) and found a host candidate ESO 601-G036. It is a low-metallicity Sc galaxy at redshift $z = 0.00867$, which is similar to that of FRB 121102. However, the chance coincidence probability is quite large, and the allowable host DM of FRB 171020 is on the lower end of FRB 121102.

So it is unclear whether FRBs in general (both repeating and nonrepeating ones) have host galaxies and subgalactic

Table 1
Parameters for FRBs with $DM_{\text{exc}} < 100 \text{ pc cm}^{-3}$

Name	Telescope	R.A. ^a	Decl.	DM pc cm^{-3}	NE2001			YMW16			ref
					DM_{MW}	DM_{halo}	DM_{exc}	DM_{MW}	DM_{halo}	DM_{exc}	
180729.J1316+55	CHIME	13:16(28.0)	+55:32(8.0)	109.6	31	30	48.6	22.75	30	56.9	1
171020 ^b	ASKAP	22:15(70.5)	−19:40(62.6)	114.1	38	30	46.1	24.71	30	59.4	2
171213 ^b	ASKAP	03:39(47.0)	−10:56(31.3)	158.6	36	30	92.6	40.69	30	87.9	2
180810.J1159+83	CHIME	11:59(172.8)	+83:07(24.9)	169.1	47	30	92.1	39.58	30	99.6	1
180814.J0422+73	CHIME	04:22:22(4.0)	+73:40(10.0)	189.4	87	30	72.4	108.07	30	51.3	3

Notes.

^a Positional uncertainties are 99% confidence limits and in units of arcminutes. The positional uncertainties of 180729.J1316+55 are given three times in CHIME/FRB Collaboration et al. (2019b), as (21′, 8′), (28′, 12′), and (28′, 8′). We use (28′, 8′) here.

^b Positional information are obtained from <https://data.csiro.au/collections/#collection/CiCSiro:34437v3>.

References. (1) CHIME/FRB Collaboration et al. (2019b); (2) Shannon et al. (2018); (3) CHIME/FRB Collaboration et al. (2019a).

environments similar to those of FRB 121102.⁶ We intend to investigate this problem by searching for host galaxy candidates of nearby FRBs (those with small DMs) in this paper. We define our nearby FRB sample in Section 2. To prepare for the host DM estimation of the candidates, we propose a galaxy-group-based method to estimate DM_{IGM} in Section 3. We then search for the nearby FRB host candidates, and compare them with the host of FRB 121102 in Section 4. We also estimate the host DM values of LGRB and SLSNe host galaxies, and compare them with those of our host candidates as well as FRB 121102 in Section 5. We draw the conclusion that the FRB 121102 host is atypical and rare. The results are summarized in Section 6 with some discussion. The following cosmological parameters have been adopted: $H_0 = 72.4 \text{ km s}^{-1} \text{ Mpc}^{-1}$, $\Omega_{\text{DM}} = 0.206$, $\Omega_{\Lambda} = 0.751$, and $\Omega_{\text{b}} = 0.043$ (Dunkley et al. 2009).

2. Sample Selection

We use the DM values of FRBs to select nearby FRBs. We decompose the total observed DM into four terms:

$$DM_{\text{tot}} = DM_{\text{MW}} + DM_{\text{halo}} + DM_{\text{IGM}} + DM_{\text{host}},$$

where DM_{MW} is the contribution from the Milky Way disk, which is estimated using the NE2001 (Cordes & Lazio 2002) or YMW16 (Yao et al. 2017) models constructed with the observed pulsar DM data; DM_{halo} is the contribution from Milky Way halo, which is estimated to be 30 pc cm^{-3} in Dolag et al. (2015) or $50\text{--}80 \text{ pc cm}^{-3}$ in Prochaska & Zheng (2019) from simulations—to be conservative, we used 30 pc cm^{-3} for our estimation; and DM_{IGM} and DM_{host} are the contributions from the intergalactic medium (IGM) and from the host galaxy, respectively. The latter also includes the contribution from the FRB local environment. We would like to use DM_{IGM} to constrain the distance, and investigate DM_{host} in this paper. We select the FRBs with the excess DM,

$$DM_{\text{exc}} = DM_{\text{tot}} - DM_{\text{MW}} - DM_{\text{halo}} \quad (1)$$

$$= DM_{\text{IGM}} + DM_{\text{host}} < 100 \text{ pc cm}^{-3}, \quad (2)$$

⁶ During the review process of this paper, the host galaxies of two more FRBs, FRB 180924 (Bannister et al. 2019) and FRB 190523 (Ravi et al. 2019) were reported, which are different from the host of FRB 121102. This is consistent with the conclusion of our paper.

from the FRBCAT catalog.⁷ There are five in total, whose basic information is listed in Table 1. The second repeating FRB discovered by CHIME/FRB Collaboration et al. (2019a), FRB 180814.J0422+73, is also on the list. We convert their positional uncertainties to the 99% confidence level based on the Gaussian distribution, which are presented in units of arcminutes in Table 1.

3. IGM DM

In order to investigate the allowable redshift range, and estimate the host DM, a relation between redshift and DM_{IGM} , i.e., $DM_{\text{IGM}} = fz$, is usually applied (Ioka 2003; Inoue 2004; Deng & Zhang 2014; Zhang 2018a), with f in the range of $\sim 850\text{--}1200 \text{ pc cm}^{-3}$. However, the relation between DM_{IGM} and redshift suffers from large uncertainties. Cosmological simulations reveal that the line-of-sight fluctuations dominate the DM_{IGM} uncertainties. The difference resulting from different lines of sight can be substantial (McQuinn 2014; Jaroszynski 2019; Pol et al. 2019).

In order to eliminate the line-of-sight uncertainty, here we propose to directly use the observed galaxy group information to estimate the cosmic density field, and hence DM_{IGM} , along the lines of sight of FRBs in our sample.

With the observed galaxy groups, Wang et al. (2009, 2016a) developed a halo-domain method to reconstruct the cosmic density field. However, Wang et al. (2016a) only covered the SDSS DR7 region, which contains only one of our object, FRB 180729.J1316+55. We therefore use a nearly all-sky galaxy-group catalog in Lim et al. (2017). To the first-order estimate, we adopt the empirical Navarro–Frenk–White (NFW) dark matter density profile (Navarro et al. 1997) to reconstruct the cosmic density field.

There are four galaxy group catalogs in Lim et al. (2017), which are produced with the galaxy catalogs from the 2MASS redshift survey (2MRS), 6dF Galaxy Survey (6dFGS), Sloan Digital Sky Survey (SDSS), and 2dF Galaxy Redshift Survey (2dFGRS). Among them, 2MRS has 91% sky coverage, nearly all except the galactic plane. Most of our FRBs are only covered by 2MRS so we use the 2MRS catalog here. However, redshift is not a good indicator of distance for nearby galaxies. We thus update the distance of the galaxies with the nearby galaxy catalog of Karachentsev et al. (2013), and then propagate the updated distances to the corresponding groups.

⁷ www.frbcatalog.org

Note that 2MRS is not complete for $z > 0.033$ (Tully 2015). The DM_{IGM} with $z > 0.033$ is only a lower limit of DM.

For each of the galaxy groups, Lim et al. (2017) estimated their dark matter halo masses, $\log M_h (M_\odot h^{-1})$. For each dark matter halo, we estimate the dark matter density profile as

$$\rho(r) = \frac{\rho_0}{(r/R_s)(1 + r/R_s)^2}, \quad (3)$$

where r is the distance from the center. $R_s = r_{200}/c_{200}$ is a scale radius. r_{200} is the radius where the average density of the halo is 200 times of cosmic critical density, $\rho_c = 3H^2/8\pi G$; c_{200} is the concentration of the halo, depending the halo mass and redshift, and we use $\log c_{200} = 0.830 - 0.098 \log M_h$ from Macciò et al. (2008). The normalization is $\rho_0 = M_h / \{4\pi R_s^3 [\ln(1+c) - c/(1+c)]\}$. However, the observational group catalog is flux limited. Wang et al. (2009, 2016a) revealed that halos with masses smaller than $10^{12} M_\odot h^{-1}$ continue smoothly to the background density of 0.2 times the mean mass density ($\rho_m = \Omega_m \rho_c = 2.45 \times 10^{-30} \text{ g cm}^{-3}$ for $h = 0.724$) of the universe, where Ω_m is the normalized mass density. We thus limit our galaxy groups to those with halo masses larger than $10^{12} M_\odot h^{-1}$, and consider $\rho = 0.2\rho_m$ as the background density in the intergalactic space in addition to the NFW density profile for the groups.

We convert the dark matter mass density ρ to baryon mass density by the ratio between Ω_b and Ω_{dm} , the normalized baryon and dark matter mass densities. If the baryon in the IGM traces dark matter and is composed of totally ionized hydrogen and helium, then the free electron number density n_e can be related to the dark matter density ρ by

$$n_e = \rho \frac{\Omega_b}{\Omega_{\text{dm}}} \left(\frac{Y_{\text{H}}}{m_{\text{H}}} + 2 \frac{Y_{\text{He}}}{m_{\text{He}}} \right) = \rho \frac{\Omega_b}{\Omega_{\text{dm}}} \frac{0.875}{m_{\text{H}}} \quad (4)$$

$$= 2.73 \times 10^{-7} \text{ cm}^{-3} \frac{\rho}{\rho_m}, \quad (5)$$

where $Y_{\text{H}} = 0.75$ and $Y_{\text{He}} = 0.25$ are the mass fractions of hydrogen and helium, and m_{H} and m_{He} are the masses of their atoms.

The electron density as a function of redshift for our nearby FRBs is presented in Figure 1. The red curve represents the electron density n_e as a function of distance (redshift) at the center of the positional region for each FRB. The yellow lines represent other 11×11 lines of sight within the positional uncertainties of each FRB. The black curve shows DM_{IGM} as a function of redshift at the center of the position uncertainty. The gray lines are again for other lines of sight within the positional uncertainties. The $DM_{\text{IGM}} = 855z \text{ pc cm}^{-3}$ relation (Zhang 2018a) is also plotted as the dashed line for comparison. It can be seen that for individual FRB sources, DM_{IGM} can be much deviated from the average value. The line of sight of FRB 180729.J1316+55 goes through a massive galaxy group around redshift 0.04. Its DM_{IGM} reaches much more than predicted by the empirical $DM_{\text{IGM}} = 855z \text{ pc cm}^{-3}$ relation at around $z = 0.05$. The largest redshift of its host galaxy is around 0.05. The center lines of sight of FRB 171020, FRB 171213, and FRB 180810.J1159+83 only go through the edge of their respective galaxy groups. Therefore, there are only small peaks in their electron density curves, and their DM_{IGM} values are smaller than the dashed line. However,

because their positional uncertainties are large, it is still possible that their lines of sight indeed pass through galaxy groups or even the center of the groups. In such cases, their DM_{IGM} values are boosted a lot, even higher than 100 pc cm^{-3} . The line of sight of FRB 180814.J0422+73, the second repeating FRB, goes through many galaxy groups within $z = 0.02$. Its DM_{IGM} is larger than the value from the $DM_{\text{IGM}} = 855z$ relation even if the 2MRS catalog is incomplete. Its DM_{IGM} reaches DM_{exc} around $z = 0.01$, indicating that its host is likely extremely nearby.

For comparison, We have also examined FRB 121102. However, FRB 121102 is too close to the Galactic plane, with a galactic latitude -0.2° . This region is avoided by most galaxy group catalogs. So, we are unable to constrain its DM_{IGM} .

To compare with other cosmological results, we calculate DM_{IGM} for different redshifts and all sky, with 360 bins in R. A., and 180 bins in decl. The distribution of the DM_{IGM} as a function of redshift z is plotted in the lowest right panel of Figure 1. The black thick curve indicates the median value for each redshift, and the gray curve presents its mean value. The orange and yellow regions show the 68% and 90% confidence levels, respectively. The black dashed curve is again the $DM_{\text{IGM}} = 855z$ relation. It turns out that the median and mean values bracket the $DM_{\text{IGM}} = 855z$ relation with $z < 0.033$, and follows nearly the same shape. It indicates that our result is generally consistent with previous rough estimation by Zhang (2018a), and our 2MRS galaxy group sample is generally complete at $z < 0.033$. However, our results flatten when reaching redshift 0.04 due to the incompleteness of 2MRS at higher redshifts. Thus, our estimation should be considered as the lower limit for $z > 0.033$.

Even without knowing the true redshift, our analysis gives a relation between DM_{IGM} and z for individual FRBs with certain uncertainties. With such a preparation, we can then estimate the values of the host DM, i.e., $DM_{\text{host}} = DM_{\text{exc}} - DM_{\text{IGM}}$, of each FRB for different redshifts. For $z > 0.033$, our derived DM_{host} can be regarded as the upper limits. These derived values can be then compared with that of FRB 121102 (see Section 4).

4. Host Galaxy Candidates

We search for host galaxy candidates using R.A., decl. of each FRB and its 99% errors. For FRB 171020 and FRB 171213, the localization probability images provided by Shannon et al. (2018) are employed. Since our FRBs are expected to be nearby, we first explore the Galaxy List for the Advanced Detector Era (GLADE) catalog (Dálya et al. 2018). It is a nearby galaxy catalog aiming at providing host galaxy candidates to gravitational wave events. It combines the galaxies in the Gravitational Wave Galaxy Catalog (White et al. 2011), 2MASS Photometric redshift catalog (2MPZ; Bilicki et al. 2014),⁸ 2MASS extended source catalog (2MASS XSC; Skrutskie et al. 2006), HyperLEDA (Makarov et al. 2014), and SDSS-DR12Q (Pâris et al. 2017). For each host candidate, we double check the redshift information in SDSS⁹ and NED.¹⁰

⁸ <http://ssa.roe.ac.uk/TWOMPZ.html>

⁹ <http://skyserver.sdss.org/dr15/en/tools/chart/navi.aspx>

¹⁰ <http://ned.ipac.caltech.edu>

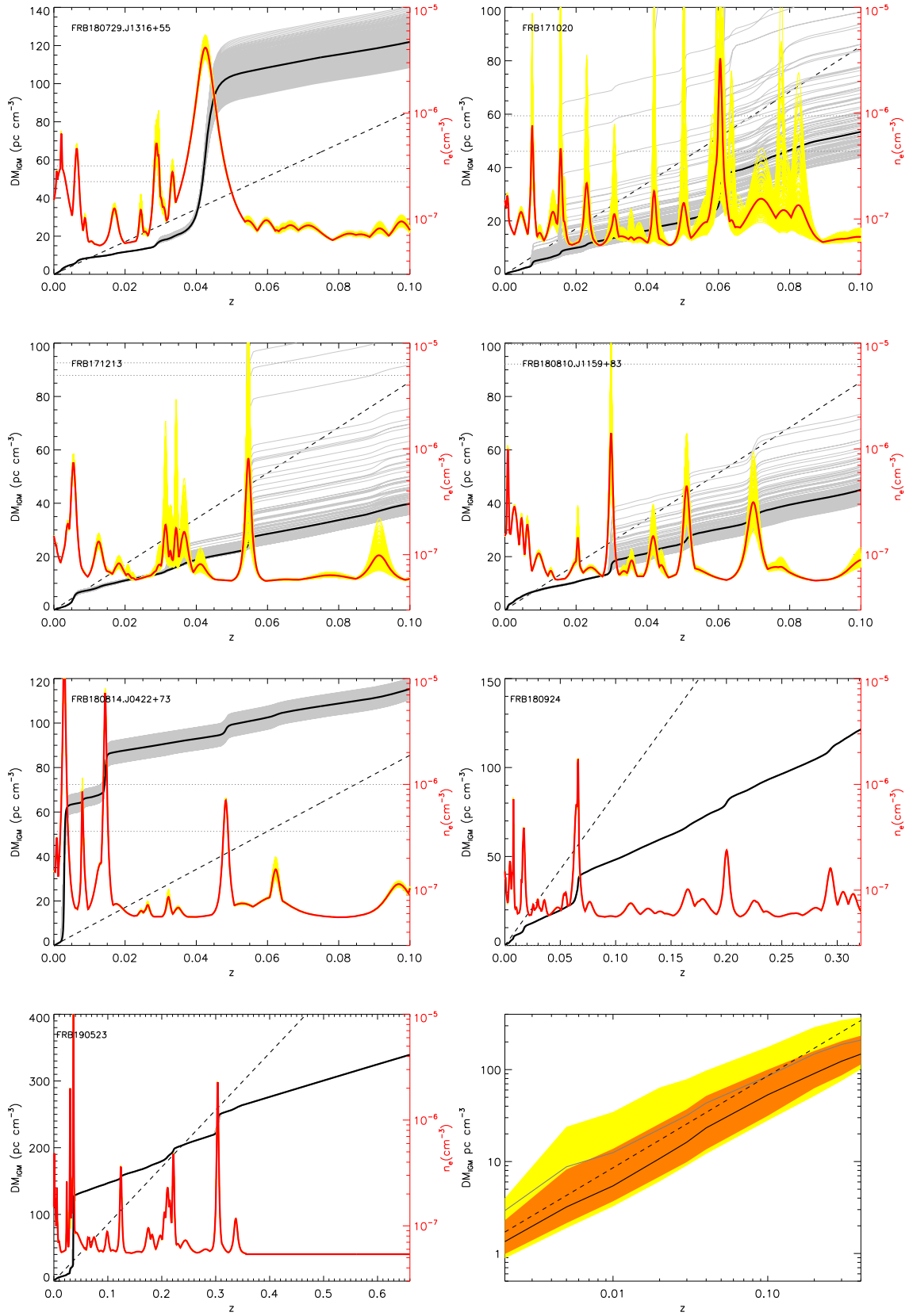


Figure 1. DM_{IGM} (black and gray lines) and electron density (red and yellow lines) as a function of redshift estimated with the galaxy group catalogs. The thick black lines and thick red lines are for the positional center of each FRB. Yellow and gray lines show the values for difference positions within the positional uncertainty for each FRB. The empirical $DM_{IGM} = 855z \text{ pc cm}^{-3}$ relation is presented as the dashed line for comparison. The range of DM_{exc} is shown as the horizontal dotted lines. Lowest right panel: the distribution of DM_{IGM} as a function of z . The black thick line and the gray thick line are the median and mean values. Orange and yellow areas are 68% and 90% regions, respectively. Again, the empirical $DM_{IGM} = 855z \text{ pc cm}^{-3}$ relation is presented as the dashed line.

Table 2
Parameters for Host Galaxy Candidates with Redshift Measurements

Name	R.A.	Decl.	Redshift	DM _{I_{GM}}	DM _{host,NE2001}	DM _{host,yw16}	m_g	M_B
FRB 180729.J1316+55	7/59/695							
SDSS J131613.66+553741.5	199.05799	55.63030	0.0270	13.9	34.7	43.0	16.7	-18.7
2MASS J13170558+5529488	199.27356	55.49705	0.0394	28.4	20.2	28.5	17.0	-19.1
SDSS J131436.14+553530.2	198.65062	55.59173	0.0810	115.3	17.8	-19.9
SDSS J131440.13+552402.8	198.66723	55.40073	0.0827	115.8	17.7	-20.1
2MASS J13144317+5535576	198.67964	55.59920	0.1138	131.6	18.2	-20.3
SDSS J131539.49+552817.0	198.91455	55.47140	0.1193	136.4	18.2	-20.4
SDSS J131720.0+553021.2	199.33329	55.50588	0.1247	141.0	22.0	-16.7
FRB 171020	12/31/4974							
ESO 601- G 036	333.85350	-19.58519	0.0087	5.1	41.0	54.3	15.2	-17.7
2MASS J22172928-1954557	334.37205	-19.91542	0.0514	20.6	25.5	38.8	16.5	-20.3
2MASS J22131992-2002022	333.33304	-20.03384	0.0619 ^a	37.3	8.8	22.1	16.5	-20.6
2MASS J22171676-1901556	334.31987	-19.03206	0.0628	37.9	8.2	21.5	16.2	-21.0
2MASS J22165509-1934325	334.22969	-19.57576	0.0632 ^a	38.0	8.1	21.4	17.0	-20.2
2MASS J22150112-1925373	333.75481	-19.42699	0.0666	39.3	6.8	20.1	16.3	-21.1
2MASS J22161241-1909585	334.05162	-19.16632	0.0832 ^a	48.2	...	11.2	17.3	-20.5
2MASS J22160049-1900395	334.00186	-19.01089	0.0923 ^a	51.2	...	8.2	17.2	-20.9
2MASS J22164473-1903516	334.18648	-19.06445	0.0925 ^a	51.2	...	8.2	17.0	-21.1
2MASS J22132225-1947211	333.34281	-19.78928	0.1030 ^a	56.0	...	3.4	17.5	-20.8
2MASS J22153780-2033247	333.90750	-20.55684	0.1074 ^a	59.8	17.3	-21.1
2MASS J22145283-2008131	333.72019	-20.13693	0.1378 ^a	85.7	18.0	-20.9
FRB 171213	5/8/1963							
2MASS J03412673-1031406	55.36138	-10.52779	0.1059 ^a	44.9	47.7	43.0	17.4	-21.1
2MASS J03383757-1109423	54.65652	-11.16177	0.1368 ^a	71.2	21.4	16.7	17.1	-22.0
2MASS J03414775-1026428	55.44890	-10.44525	0.1400 ^a	73.9	18.7	14.0	17.9	-21.2
2MASS J03385211-1058563	54.71704	-10.98223	0.1406 ^a	74.5	18.1	13.4	18.4	-20.8
2MASS J03382824-1104255	54.61758	-11.07368	0.1409 ^a	74.7	17.9	13.2	18.1	-21.0
FRB 180810.J1159+83	3/3/1066							
2MASS J11552291+8246314	178.84550	82.77529	0.0438 ^a	23.0	69.1	76.5	16.6	-20.4
2MASS J12045319+8322007	181.22218	83.36675	0.0816 ^a	39.9	52.2	59.7	17.7	-20.6
2MASS J11595630+8301545	179.98360	83.03170	0.1203 ^a	62.4	29.7	37.1	18.3	-20.9
FRB 180814.J0422+73	1/1/50							
2MASS J04222144+7347101	65.58900	73.78612	0.0781 ^a	108.3	17.5	-20.6

Note.

^a Photometric redshift from 2MPZ.

In order to be more complete, we also explore the extended sources in the Pan-STARRS catalog¹¹ (Chambers et al. 2016; Flewelling et al. 2016). Following the menu of Pan-STARRS, we select objects in the StackObjectThin database table, exclude spurious sources by requiring $ndetections > 1$, and select Pan-STARRS galaxies by requiring $mag_{PSF} - mag_{Kron} > 0.05$. We find and delete duplicate objects whose coordinates are off by $1''$. We then assign redshifts from SDSS, 2MPZ, and NED to Pan-STARRS sources, allowing a coordinate offset by $3''$.

We use R.A., decl., and their 99% errors to select host galaxy candidates. For FRB 171020 and FRB 171213, we use the localization probability images provided by Shannon et al. (2018) to select the galaxy candidates. The candidates with redshifts, spectroscopic or photometric, less than 0.15 are presented in Table 2. The numbers after the FRB names give the number of galaxies with redshift less than 0.15, the number

of galaxies with redshifts, and the total number of galaxies (most of them are Pan-STARRS extended sources). For each of the candidates, we estimate the expected $DM_{host} = DM_{exc} - DM_{IGM}$ for NE2001 and YMW16, respectively, as $DM_{host,NE2001}$ and $DM_{host,yw16}$. For those with redshift $z > 0.1$, the DM_{IGM} is estimated by requiring $\Delta DM_{IGM} = 855 \Delta z$ for $z > 0.1$, and following Figure 1 for $z < 0.1$. With their g -band Kron magnitude (when available), or g -band point-spread function magnitudes, presented as m_g , we estimate their B -band absolute magnitude M_B following

$$M_B = m_g - A_g - 5 \log \left(\frac{D_L}{10 \text{pc}} \right) - 2.5(\beta + 2) \log \left[\frac{(1+z)\lambda_0}{\lambda} \right] + 2.5 \log(1+z)$$

(Laskar et al. 2011), where A_g is the Galactic extinction in g band, D_L is luminosity distance, and z is the redshift, λ is the observational effective wavelength, 4900 Å for PanSTARRS g band, λ_0 is the rest frame effective wavelength, 4300 Å for B band, and β is the index of the assumed power-law spectrum,

¹¹ <https://outerspace.stsci.edu/display/PANSTARRS>

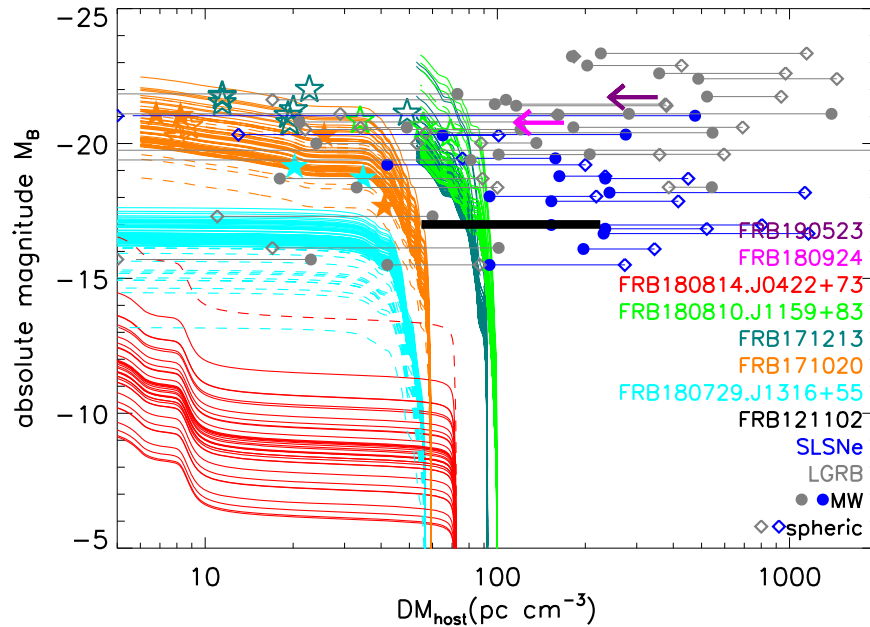


Figure 2. B band absolute magnitudes M_B vs. DM_{host} . Candidates for different FRBs are plotted with different colors. Filled stars indicate candidates with spectroscopic redshifts. For FRB candidates without redshift information, we assume different redshifts in 0–0.1 to calculate their M_B and DM_{host} , and plot them as solid lines. Candidates with photometric redshifts are presented as open stars, and they are also plotted as dashed lines for different assumed redshifts. For comparison, FRB 121102 is plotted as a thick black solid line. FRB 180924 and FRB 190523 are presented as magenta and purple arrows. Their DM_{host} are estimated based on the estimation of DM_{IGM} . LGRB and SLSNe host galaxies are denoted as gray and blue symbols. Filled dots are for the MW template, and diamonds are for the spherical electron density profile.

$F_\lambda \propto \lambda^\beta$. Because we examine blue/green bands and the expected spectrum of FRB 121102 host may be similar to GRB hosts, we adopt $\beta = -2.3$ following Laskar et al. (2011). Their g -band magnitude and absolute magnitudes M_B are also presented.

The candidates are compared with the host of FRB 121102 in a DM_{host} versus absolute magnitude M_B diagram (Figure 2). Tendulkar et al. (2017) estimated the DM_{host} of FRB 121102 to be $DM_{\text{host}} = 140 \pm 85 \text{ pc cm}^{-3}$, by an empirically estimated DM_{IGM} , with an error of 85 pc cm^{-3} . Kokubo et al. (2017) gives $DM_{\text{host}} = 163 \pm 96 \text{ pc cm}^{-3}$ by taking the uncertainty of MW, IGM and observation into account. We thus use $55 < DM_{\text{host}} < 225 \text{ pc cm}^{-3}$ to be conservative, and presented it as the black thick line. Candidates for different FRBs are represented by different colors. Candidates with spectroscopic redshifts are plotted as filled stars, with the values in Table 2. For those without redshifts, we estimate their DM_{host} and M_B by assuming redshifts $z = 0-0.1$, following the same method in the last paragraph, and then plot them as solid curves. To be clear, we only plot the brightest 50 candidates without redshifts for each FRB. There are many more galaxies fainter than what we presented. Candidates with photometric redshifts are presented as open stars, with dashed curves indicating different redshifts also.

4.1. FRB 180729.J1316+55

There are 695 extended sources within the positional region of FRB 180729.J1316+55. Among them, 59 have spectroscopic redshifts from SDSS. There are seven galaxies with spectroscopic redshifts less than 0.15. Two of them, SDSS

J131613.66+553741.5 and 2MASS 13170558+5529488 have relatively large values of DM_{host} .¹²

The first one, SDSS J131613.66+553741.5, is a faint source within a big disk galaxy SDSS J131613.95+553749.5. It is likely a star-forming region in the galaxy. Its expected DM_{host} is 35 pc cm^{-3} and 43 pc cm^{-3} for the NE2001 and YMW16 models, respectively. The second one, SDSS 131705.58+552948.8, is an edge-on disk galaxy with a significant bulge. SED fitting gives stellar mass $M_* = 3 \times 10^{10} M_\odot$, $\text{SFR} = 0.007 M_\odot \text{ yr}^{-1}$ (Chang et al. 2015). Its expected DM_{host} are 20 pc cm^{-3} and 28 pc cm^{-3} for the NE2001 and YMW16 models, respectively. These two sources both have a smaller DM_{host} than FRB 121102. Other host galaxy candidates have even smaller DM_{host} than FRB 121102.

4.2. FRB 171020

There are 4974 extended sources within the error box of FRB 171020. Among them, 31 have redshift information. Four of them have spectroscopic redshifts smaller than 0.15, and 8 of them have photometric redshifts smaller than 0.15. The one with the lowest redshift, ESO 601-G 036, is the galaxy candidate proposed by Mahony et al. (2018). It has $DM_{\text{host}} = 41 \text{ pc cm}^{-3}$ and 54 pc cm^{-3} for NE2001 and YMW16 models, respectively. For most possible redshifts, the derived DM_{host} is much smaller than that of FRB 121102. Only if the host galaxy is intrinsically very faint (so they are much closer) could its DM_{host} reach the lower limit of FRB 121102 DM_{host} . In this case, the host galaxy candidate should have an absolute magnitude similar to or larger (fainter) than that of FRB 121102. As shown in Figure 2, galaxies without

¹² GLADE used the photometric redshift 0.06263 in the catalog. However, its SDSS spectroscopic redshift is 0.039.

redshift information may achieve $DM_{\text{host}} = 40\text{--}60 \text{ pc cm}^{-3}$ if they are extremely nearby.

4.3. FRB 171213 and FRB 180810.J1159+83

Both FRB 171213 and FRB 180810.J1159+83 have $DM_{\text{exc}} \sim 90 \text{ pc cm}^{-3}$. It is possible to find a host galaxy candidate similar to that of FRB 121102. Also, they are out of the redshift range for our galaxy-group-based method for the z - DM_{IGM} relation. We thus do not explore them in detail.

4.4. FRB 180814.J0422+73

FRB 180814.J0422+73 is the second repeating FRB (CHIME/FRB Collaboration et al. 2019a). There are only 50 extended sources found in Pan-STARRS, and 1 in GLADE in the error box. This is due to the smaller positional uncertainty compared with other objects. The brightest galaxy is the one found in GLADE, with a g -band kron magnitude 17.5 mag, and a 2MASS photometric redshift 0.078. The second brightest one is a point source with another fainter point source $1''.7$ away. It is quite likely spurious, so we do not show it in the plot. Other galaxies are more than one order of magnitude fainter than these two.

There are many galaxy groups near the line of sight of FRB 180814.J0422+73 for $z < 0.02$. The host galaxy should have to be very nearby, if they have a DM_{host} similar to that of FRB 121102. They should then be intrinsically very faint. As shown in Figure 2, the host of FRB 180814.J0422+73 has to be much fainter than -14 magnitude, more than 3 orders of magnitude fainter than that of FRB 121102, if a DM_{host} similar to that of FRB 121102 is assumed. The DM_{host} of FRB 180814.J0422+73 must be very small ($< 7 \text{ pc cm}^{-3}$), if its host is as bright as FRB 121102. In this case, the galaxy with redshift, 2MASS J042221.4+734710.2, is not the host, if its photometric redshift is correct.

Even if we use the empirical $z - DM_{\text{IGM}}$ relation, the conclusion is similar. If 2MASS J042221.4+734710.2 is the host galaxy of FRB 180814.J0422+73, the estimated $DM_{\text{IGM}} = 67 \text{ pc cm}^{-3}$ (Deng & Zhang 2014), indicating $DM_{\text{host}} \sim 5 \text{ pc cm}^{-3} DM$. If 2MASS J042221.4+734710.2 is not the host, the host galaxy should be at least three orders of magnitude fainter than the host of FRB 121102, that is, $M_r > -14$ mag. For comparison, LMC and SMC have absolute magnitudes -18.36 and -16.82 , respectively. In this case, the FRB would be quite local although still extragalactic. Its isotropic energy would have to be two or three orders of magnitude smaller than typical FRBs, e.g., FRB 121102.

In general, we conclude that the host galaxies of nearby FRBs typically have small DM_{host} values, or are intrinsically faint, much fainter than the hosts of LGRBs and SLSNe (Metzger et al. 2017). This is in contrast to the conclusion drawn from the FRB 121102 measurement (Kokubo et al. 2017; Tendulkar et al. 2017) and the statistical analysis of Yang et al. (2017). Future observations of more localized FRBs will test whether a small DM_{host} is typical for nearby FRBs only or for most FRBs in general.

5. DM Contribution from the Host Galaxies of LGRBs and SLSNe

Due to the similarity of the FRB 121102 host with LGRB/SLSNe hosts, FRBs are highly believed to be powered by magnetars born during LGRBs and SLSNe (Bassa et al. 2017;

Kashiyama & Murase 2017; Metzger et al. 2017; Nicholl et al. 2017). We want to further explore whether the host galaxies of nearby FRBs are similar to those of LGRBs and SLSNe.

Host galaxies of LGRBs and SLSNe are generally star-forming dwarf galaxies (Sahu et al. 1997; Bloom et al. 1998, 2002; Chary et al. 2002; Christensen et al. 2004; Savaglio et al. 2009; Krühler et al. 2015). If the galaxy electron density is known, the host galaxy DM contribution can be estimated based on the scale length r_e , and the offset of the transient from the center of the galaxy r_{off} (Bloom et al. 2002; Fruchter et al. 2006; Blanchard et al. 2016; Li et al. 2016).

The free electrons in the interstellar medium are generally ionized by the death of massive stars. They are thus likely correlated to the star formation rate (SFR) and $H\alpha$ emission (Reynolds 1977; Luo et al. 2018). We can thus estimate their electron density n_e based on their $H\alpha$ emission lines, or SFR. Since resolved optical emission is not always available, we test two possible distributions, i.e., the spherical Gaussian distribution and Milky Way-like distribution.

We obtained SFR, r_e , r_{off} and absolute magnitude of SLSNe from Lunnan et al. (2015), Schulze et al. (2018), and Perley et al. (2016), and those of LGRBs from Li et al. (2016). We then estimate the DM_{host} from LGRBs/SLSNe-like host galaxies as follows.

5.1. Spherical Gaussian Distribution

LGRB and SLSN hosts are dwarf star-forming galaxies, which resemble SMC in many aspects. Following the treatment of SMC by Yao et al. (2017), we assume that the electron density follows

$$n_e = n_0 e^{-(r/r_e)^2},$$

where r_e is the scale length of the galaxy.

Since LGRBs and SLSNe both highly trace massive stars, it is reasonable to assume that they are in the disk plane. If the host is face on, for a specific offset r_{off} , one has

$$\begin{aligned} DM &\equiv \int_0^\infty n_e dl = \frac{\sqrt{\pi}}{2} n_0 r_e \exp\left(-\frac{r_{\text{off}}^2}{r_e^2}\right), \\ EM &\equiv \int_{-\infty}^\infty n_e^2 dl = \sqrt{\frac{\pi}{2}} n_0^2 r_e \exp\left(-2\frac{r_{\text{off}}^2}{r_e^2}\right), \end{aligned}$$

so that

$$DM^2 = \sqrt{\frac{\pi}{8}} r_e EM.$$

According to Reynolds (1977), $H\alpha$ surface density is a tracer of EM, i.e.,

$$EM = 2.75 \left(\frac{T}{10^4 \text{ K}}\right)^{0.9} \frac{\Sigma_{H\alpha}}{2.42 \times 10^{-7} \text{ erg s}^{-1} \text{ cm}^{-2} \text{ sr}^{-1}} \text{ cm}^{-6} \text{ p} \quad (6)$$

$$= 486 \left(\frac{T}{10^4 \text{ K}}\right)^{0.9} \frac{\Sigma_{H\alpha}}{10^{-15} \text{ erg s}^{-1} \text{ cm}^{-2} \text{ arcsec}^{-2}} \text{ cm}^{-6} \text{ pc}. \quad (7)$$

If the $H\alpha$ surface density follows the distribution of EM relative to r_{off} , one then has

$$\Sigma_{H\alpha}(r) = \Sigma_{H\alpha 0} \exp\left(-2\frac{r_{\text{off}}^2}{r_e^2}\right),$$

and the $H\alpha$ flux can be written as

$$F_{H\alpha} = \int_0^\infty \int_0^{2\pi} \Sigma_{H\alpha 0} \exp\left(-2\frac{r^2}{r_e^2}\right) r dr d\theta = \frac{\pi r_e^2}{2} \Sigma_{H\alpha 0}.$$

Combining the relations among DM, EM, $\Sigma_{H\alpha 0}$, and $F_{H\alpha}$, one has

$$DM^2 = 486 \times 10^{15} \sqrt{\frac{\pi}{8}} r_{e,\text{pc}} \left(\frac{T}{10^4 \text{ K}}\right)^{0.9} \left(\frac{2F_{H\alpha}}{\pi r_e^2}\right) \exp\left(-2\frac{r_{\text{off}}^2}{r_e^2}\right) \quad (8)$$

where $F_{H\alpha}$ is in units of $\text{erg s}^{-1} \text{cm}^{-2}$, r_e and r_{off} are in units of arcseconds, $r_{e,\text{pc}}$ is in units of parsecs, and DM is in units of $\text{cm}^{-3} \text{pc}$.

5.2. Milky Way-like Distribution

We also consider a Milky Way-like electron density distribution as the template of a disk galaxy (Yao et al. 2017), i.e.,

$$n_0 \propto \sqrt{\frac{L_{H\alpha}}{r_e^3}}, \quad (9)$$

for each LGRB/SLSNe host galaxy. The offset is rescaled by $r'_{\text{off},\text{MW}} = \frac{r_{\text{off}}}{r_e} r_{e,\text{MW}}$. The Milky Way SFR, $\text{SFR}_{\text{MW}} = 0.27 M_\odot \text{yr}^{-1}$ (Licquia & Newman 2015), and the Milky Way scale length $r_{e,\text{MW}} = 2.15 \pm 0.14 \text{ kpc}$ (Bovy & Rix 2013) are used. The DM_{host} values estimated with this MW template are presented as blue and gray dots in Figure 2, for SLSNe and LGRBs, respectively.

5.3. Comparison between the Candidates and LGRB/SLSNe Hosts

For both spherical Gaussian distribution and MW-like distribution, the hosts of LGRBs and SLSNe contribute $\sim 100 \text{ cm}^{-3} \text{pc}$ to DM. Only $< 10\%$ of LGRBs have $DM_{\text{host}} < 30 \text{ cm}^{-3} \text{pc}$. None of the SLSNe have a $DM_{\text{host}} < 30 \text{ cm}^{-3} \text{pc}$. They are plotted in Figure 2 for comparison. Blue and gray colors are for SLSNe and LGRBs respectively. Dots and diamonds are for spherical and MW-like distributions, respectively.

FRB 121102 has an estimated DM_{host} in the range of $55\text{--}225 \text{ pc cm}^{-3}$. This is consistent with the estimated value of LGRBs and SLSNe. Also, the absolute magnitude of its host galaxy, -17 , is consistent with the values for the LGRB and SLSN host samples.

Other FRB host candidates, on the other hand, are not consistent with the LGRB and SLSN host samples. The host galaxy candidates for FRB 180729.J1316+55, FRB 171020, FRB 171213, and FRB 180814.J0422+73 all have a smaller DM_{host} than the lower limit of FRB 121102, 55 pc cm^{-3} . The host galaxy candidates of FRB 180814.J0422+73 do not overlap with either LGRBs or SLSNe at all. The host candidates of FRB 180729.J1316+55 overlap with 5 of the 37 LGRB hosts, but no SLSN host. It is located in the faint,

low DM_{host} corner of the LGRB/SLSN host distribution. FRB 171020, FRB 171213, and FRB 180810.J1159+83 pass through the DM_{host} range of LGRB and SLSN hosts, so the possibility that their hosts are LGRB/SLSN-like is not ruled out. However, All of them are located within the very low end of the LGRB/SLSN DM_{host} distribution. So, collectively, the probability that all the nearby FRB hosts are consistent with the LGRB/SLSN hosts is extremely low.

6. FRB 180924 and FRB 190523

During the review of this paper, two FRBs were located to their host galaxies. FRB 180924 was in a massive passive galaxy $z = 0.3214$ (Bannister et al. 2019), and FRB 190523 was in a massive galaxy at $z = 0.66$ (Ravi et al. 2019). Both host galaxies are unlike that of FRB 121102, supporting our conclusion that the host of FRB 121102 is atypical. On the other hand, those two host galaxies are also brighter than most of our host candidates.

In order to apply our method to these FRBs, we extend the galaxy group catalog to higher redshifts with Wen et al. (2018), which covers all of the sky except for the Galactic plane, extends to redshift 0.4, and has a median redshift 0.24. 479 galaxy groups within it are excluded because they are duplicated with the 2MRS galaxy group. The electron density and cumulative DM_{IGM} of FRB 180924 and FRB 190523 are also presented in Figure 1. The derived DM_{IGM} of FRB 180924 at redshift $z = 0.3214$ is 121 pc cm^{-3} , and that of FRB 180924 at redshift $z = 0.66$ is 339 pc cm^{-3} . However, the total halo mass range of the galaxy group sample in Wen et al. (2018) is $[7 \times 10^{13}, 2 \times 10^{15}] M_\odot$, much larger than the mass threshold $10^{12} M_\odot$ we applied. As a result, many galaxy groups are likely missed. Furthermore, our galaxy group catalogs do not extend to redshift $z > 0.4$, so we are unable to constrain the 0.4–0.66 range for FRB 190523. As a result, the DM_{IGM} obtained with our method should be considered as very loose lower limits for these two FRBs. By subtracting the DM_{MW} and $DM_{\text{halo}} = 30 \text{ pc cm}^{-3}$, one gets loose upper limits of DM_{host} for FRB 180924 and FRB 190523: $DM_{\text{host,FRB 180924}} < 169 \text{ pc cm}^{-3}$ and $DM_{\text{host,FRB 190523}} < 354 \text{ pc cm}^{-3}$, respectively.

These two FRBs are also presented in Figure 2. The very loose DM_{host} upper limits are also plotted. One can see that most host candidates of nearby FRBs are also much fainter than these two hosts. As these two hosts also differ from that of FRB 121102 in terms of SFR and offset between the FRB and the host, one can draw the conclusion that the FRB hosts are very diverse among bursts.

7. Conclusion and Discussion

We have searched the host galaxy candidates of nearby FRBs whose DM_{exc} is below 100 pc cm^{-3} . Due to the selection criteria, their DM_{host} are expected to be smaller than 100 pc cm^{-3} . The following conclusions can be drawn:

1. Not all FRBs reside in environments similar to FRB 121102. The existence of FRBs with DM_{host} less than the lower limit of FRB 121102 DM_{host} reveals that not all FRBs are located in environments similar to FRB 121102. The fact that the hosts of the recently localized FRB 180924 and FRB 190523 are also different from that of FRB 121102 and the host candidates studied in this paper strengthens our conclusion and suggests that FRB hosts are very diverse.

2. It is strengthened when we examine the DM_{host} versus M_B relation. The DM_{host} of FRB 180814.J0422+73 must be smaller than 10 pc cm^{-3} if it is a normal galaxy, or it is within a galaxy fainter than -14 mag .

2. Based on the required DM_{host} versus M_B relation, the host galaxies of FRB 180729.J1316+55, FRB 171020, and FRB 180814.J0422+73 cannot be similar to the hosts of SLSNe, and are very likely not similar to the hosts of LGRBs, either. This suggests that LGRBs and SLSNe are likely not the progenitors of most FRB sources.




3. The host galaxies of LGRBs and SLSNe typically contribute to a relatively large $DM_{\text{host}} \sim 100 \text{ pc cm}^{-3}$.

4. We develop an observational galaxy-group-based method to estimate the DM_{IGM} of FRBs. This method can directly address the line-of-sight uncertainty of the $DM-z$ relation, even though the results are only reliable up to $z = 0.033$ below which the complete galaxy group catalogs are available. Such a method can be applied to infer the distance of other nearby FRBs detected in the future.

Our results on DM_{IGM} somewhat depend on the assumed density in the intergalactic space, which we discussed in Section 3 and Equation (5). We have tested the uncertainty by assuming zero electron density for the IGM, in which case we obtain a DM that is smaller by $5\text{--}10 \text{ pc cm}^{-3}$. Therefore, our conclusions are not significantly affected by our assumption of the IGM density. In addition, the result of the cosmological hydrodynamic simulations of galaxy formation with star formation and SN feedback by the GADGET3-Osaka SPH code (Shimizu et al. 2019) suggested a comoving electron density similar to Equation (5) within a factor of a few. This also corroborates that the electron density value in Equation (5) is fairly reasonable.

We thank the referee for the helpful suggestions. Y.L. thanks Seunghwan Lim, Huiyuan Wang, Weiwei Xu, and Qiang Yuan for helpful discussions. Y.L. is supported by the KIAA-CAS Fellowship, which is jointly supported by Peking University and Chinese Academy of Sciences. This work is also partially supported by the China Postdoctoral Science Foundation (No. 2018M631242). K.N. acknowledges the support by the JSPS KAKENHI grant No. JP17H01111, and the Kavli IPMU, World Premier Research Center Initiative (WPI). J.J.S. is supported by the Boya Fellowship.

ORCID iDs

Ye Li  <https://orcid.org/0000-0001-5931-2381>
 Bing Zhang  <https://orcid.org/0000-0002-9725-2524>
 Kentaro Nagamine  <https://orcid.org/0000-0001-7457-8487>

References

- Akiyama, K., & Johnson, M. D. 2016, *ApJL*, 824, L3
 Bannister, K. W., Deller, A. T., Phillips, C., et al. 2019, *Sci*, 365, 6453
 Bassa, C. G., Tendulkar, S. P., Adams, E. A. K., et al. 2017, *ApJL*, 843, L8
 Belorodov, A. M. 2017, *ApJL*, 843, L26
 Bilicki, M., Jarrett, T. H., Peacock, J. A., Cluver, M. E., & Steward, L. 2014, *ApJS*, 210, 9
 Blanchard, P. K., Berger, E., & Fong, W.-F. 2016, *ApJ*, 817, 144
 Bloom, J. S., Djorgovski, S. G., Kulkarni, S. R., & Frail, D. A. 1998, *ApJL*, 507, L25
 Bloom, J. S., Kulkarni, S. R., & Djorgovski, S. G. 2002, *AJ*, 123, 1111
 Bovy, J., & Rix, H.-W. 2013, *ApJ*, 779, 115
 Caleb, M., Stappers, B. W., Rajwade, K., & Flynn, C. 2019, *MNRAS*, 484, 5500
 Chambers, K. C., Magnier, E. A., Metcalfe, N., et al. 2016, arXiv:1612.05560
 Chang, Y.-Y., van der Wel, A., da Cunha, E., & Rix, H.-W. 2015, *ApJS*, 219, 8
 Chary, R., Becklin, E. E., & Armus, L. 2002, *ApJ*, 566, 229
 Chatterjee, S., Law, C. J., Wharton, R. S., et al. 2017, *Natur*, 541, 58
 CHIME/FRB Collaboration, Amiri, M., Bandura, K., et al. 2019a, *Natur*, 566, 235
 CHIME/FRB Collaboration, Amiri, M., Bandura, K., et al. 2019b, *Natur*, 566, 230
 Christensen, L., Hjorth, J., & Gorosabel, J. 2004, *A&A*, 425, 913
 Connor, L., Sievers, J., & Pen, U.-L. 2016, *MNRAS*, 458, L19
 Cordes, J. M., & Lazio, T. J. W. 2002, arXiv:astro-ph/0207156
 Cordes, J. M., & Wasserman, I. 2016, *MNRAS*, 457, 232
 Dai, Z. G. 2019, *ApJL*, 873, L13
 Dai, Z. G., Wang, J. S., Wu, X. F., & Huang, Y. F. 2016, *ApJ*, 829, 27
 Dályá, G., Galgóczi, G., Dobos, L., et al. 2018, *MNRAS*, 479, 2374
 Deng, W., & Zhang, B. 2014, *ApJL*, 783, L35
 Dolag, K., Gaensler, B. M., Beck, A. M., & Beck, M. C. 2015, *MNRAS*, 451, 4277
 Dunkley, J., Komatsu, E., Nolta, M. R., et al. 2009, *ApJS*, 180, 306
 Falcke, H., & Rezzolla, L. 2014, *A&A*, 562, A137
 Flewelling, H. A., Magnier, E. A., Chambers, K. C., et al. 2016, arXiv:1612.05243
 Fruchter, A. S., Levan, A. J., Strolger, L., et al. 2006, *Natur*, 441, 463
 Geng, J. J., & Huang, Y. F. 2015, *ApJ*, 809, 24
 Inoue, S. 2004, *MNRAS*, 348, 999
 Ioka, K. 2003, *ApJL*, 598, L79
 Jaroszynski, M. 2019, *MNRAS*, 484, 1637
 Johnston, S., Keane, E. F., Bhandari, S., et al. 2017, *MNRAS*, 465, 2143
 Karachentsev, I. D., Makarov, D. I., & Kaisina, E. I. 2013, *AJ*, 145, 101
 Kashiyama, K., Ioka, K., & Mészáros, P. 2013, *ApJL*, 776, L39
 Kashiyama, K., & Murase, K. 2017, *ApJL*, 839, L3
 Katz, J. I. 2016, *ApJ*, 818, 19
 Keane, E. F., Johnston, S., Bhandari, S., et al. 2016, *Natur*, 530, 453
 Kokubo, M., Mitsuda, K., Sugai, H., et al. 2017, *ApJ*, 844, 95
 Krühler, T., Malesani, D., Fynbo, J. P. U., et al. 2015, *A&A*, 581, A125
 Laskar, T., Berger, E., & Chary, R.-R. 2011, *ApJ*, 739, 1
 Li, Y., & Zhang, B. 2016, arXiv:1603.04825
 Li, Y., Zhang, B., & Lü, H.-J. 2016, *ApJS*, 227, 7
 Licquia, T. C., & Newman, J. A. 2015, *ApJ*, 806, 96
 Lim, S. H., Mo, H. J., Lu, Y., Wang, H., & Yang, X. 2017, *MNRAS*, 470, 2982
 Liu, T., Romero, G. E., Liu, M.-L., & Li, A. 2016, *ApJ*, 826, 82
 Lorimer, D. R. 2018, *NatAs*, 2, 860
 Lorimer, D. R., Bailes, M., McLaughlin, M. A., Narkevic, D. J., & Crawford, F. 2007, *Sci*, 318, 777
 Lunnan, R., Chornock, R., Berger, E., et al. 2015, *ApJ*, 804, 90
 Luo, R., Lee, K., Lorimer, D. R., & Zhang, B. 2018, *MNRAS*, 481, 2320
 Macciò, A. V., Dutton, A. A., & van den Bosch, F. C. 2008, *MNRAS*, 391, 1940
 Mahony, E. K., Ekers, R. D., Macquart, J.-P., et al. 2018, *ApJL*, 867, L10
 Makarov, D., Prugniel, P., Terekhova, N., Courtois, H., & Vauglin, I. 2014, *A&A*, 570, A13
 Marcote, B., Paragi, Z., Hessels, J. W. T., et al. 2017, *ApJL*, 834, L8
 McQuinn, M. 2014, *ApJL*, 780, L33
 Metzger, B. D., Berger, E., & Margalit, B. 2017, *ApJ*, 841, 14
 Metzger, B. D., Margalit, B., & Sironi, L. 2019, *MNRAS*, 485, 4091
 Navarro, J. F., Frenk, C. S., & White, S. D. M. 1997, *ApJ*, 490, 493
 Nicholl, M., Williams, P. K. G., Berger, E., et al. 2017, *ApJ*, 843, 84
 Palaniswamy, D., Li, Y., & Zhang, B. 2018, *ApJL*, 854, L12
 Pâris, I., Petitjean, P., Ross, N. P., et al. 2017, *A&A*, 597, A79
 Perley, D. A., Quimby, R. M., Yan, L., et al. 2016, *ApJ*, 830, 13
 Petroff, E., Barr, E. D., Jameson, A., et al. 2016, *PASA*, 33, e045
 Piro, A. L. 2012, *ApJ*, 755, 80
 Pol, N., Lam, M. T., McLaughlin, M. A., Lazio, T. J. W., & Cordes, J. M. 2019, arXiv:1903.07630
 Prochaska, J. X., & Zheng, Y. 2019, *MNRAS*, 485, 648
 Ravi, V., Catha, M., D'Addario, L., et al. 2019, *Natur*, 572, 352
 Reynolds, R. J. 1977, *ApJ*, 216, 433
 Sahu, K. C., Livio, M., Petro, L., et al. 1997, *Natur*, 387, 476
 Savaglio, S., Glazebrook, K., & Le Borgne, D. 2009, *ApJ*, 691, 182
 Schulze, S., Krühler, T., Leloudas, G., et al. 2018, *MNRAS*, 473, 1258
 Shannon, R. M., Macquart, J.-P., Bannister, K. W., et al. 2018, *Natur*, 562, 386
 Shimizu, I., Todoroki, K., Yajima, H., & Nagamine, K. 2019, *MNRAS*, 484, 2632
 Skrutskie, M. F., Cutri, R. M., Stiening, R., et al. 2006, *AJ*, 131, 1163
 Spitler, L. G., Cordes, J. M., Hessels, J. W. T., et al. 2014, *ApJ*, 790, 101
 Spitler, L. G., Scholz, P., Hessels, J. W. T., et al. 2016, *Natur*, 531, 202
 Tendulkar, S. P., Bassa, C. G., Cordes, J. M., et al. 2017, *ApJL*, 834, L7

- Thornton, D., Stappers, B., Bailes, M., et al. 2013, *Sci*, 341, 53
- Totani, T. 2013, *PASJ*, 65, L12
- Tully, R. B. 2015, *AJ*, 149, 171
- Vedantham, H. K., Ravi, V., Mooley, K., et al. 2016, *ApJL*, 824, L9
- Wang, H., Mo, H. J., Jing, Y. P., et al. 2009, *MNRAS*, 394, 398
- Wang, H., Mo, H. J., Yang, X., et al. 2016a, *ApJ*, 831, 164
- Wang, J.-S., Yang, Y.-P., Wu, X.-F., Dai, Z.-G., & Wang, F.-Y. 2016b, *ApJL*, 822, L7
- Wen, Z. L., Han, J. L., & Yang, F. 2018, *MNRAS*, 475, 343
- White, D. J., Daw, E. J., & Dhillon, V. S. 2011, *CQGra*, 28, 085016
- Williams, P. K. G., & Berger, E. 2016, *ApJL*, 821, L22
- Yang, Y.-P., Luo, R., Li, Z., & Zhang, B. 2017, *ApJL*, 839, L25
- Yao, J. M., Manchester, R. N., & Wang, N. 2017, *ApJ*, 835, 29
- Zhang, B. 2014, *ApJL*, 780, L21
- Zhang, B. 2016, *ApJL*, 827, L31
- Zhang, B. 2017, *ApJL*, 836, L32
- Zhang, B. 2018a, *ApJL*, 867, L21
- Zhang, B. 2018b, *ApJL*, 854, L21
- Zhang, B. 2019, *ApJL*, 873, L9